

Somatostatin Receptors in Malignant Lymphomas: Targets for Radiotherapy?

Virgil A.S.H. Dalm, PhD¹; Leo J. Hofland, PhD¹; Cornelia M. Mooy, MD, PhD²; Marlijn A. Waaijers¹; Peter M. van Koetsveld¹; Anton W. Langerak, PhD³; Frank T.J. Staal, PhD³; Aart-Jan van der Lely, MD, PhD¹; Steven W.J. Lamberts, MD, PhD¹; and Martin P. van Hagen, MD, PhD^{1,3}

¹Department of Internal Medicine, Erasmus Medical Center, Rotterdam, The Netherlands; ²Department of Ophthalmic Pathology, Erasmus Medical Center, Rotterdam, The Netherlands; and ³Department of Immunology, Erasmus Medical Center, Rotterdam, The Netherlands

Somatostatin (SS) receptor (sst) scintigraphy is widely used in the visualization of neuroendocrine tumors expressing sst, and radiotherapy using radionuclide-labeled SS analogs has been introduced for treatment of patients with neuroendocrine tumors. Previous sst scintigraphy studies revealed that malignant lymphomas can also be visualized using this technique. The question has been addressed whether lymphomas might also be possible targets for radiotherapy using radionuclide-labeled SS analogs. Therefore, we investigated in vitro the characteristics of lymphoma tissues and lymphoid cell lines to evaluate whether lymphomas can be targets for radiotherapy. **Methods:** Six orbital lymphomas, 2 Hodgkin's lymphomas, and 2 non-Hodgkin's lymphomas from the neck region were collected. Reverse transcriptase polymerase chain reaction (RT-PCR) and quantitative RT-PCR were performed to detect and quantify the expression of sst₁₋₅ mRNA. Receptor autoradiography studies using [¹²⁵I-Tyr³]octreotide were performed to evaluate binding to sst on cryostat sections of lymphomas. Immunohistochemistry was used to investigate expression of sst₂ and sst₃. Membrane binding studies and in vitro internalization experiments using [¹²⁵I-Tyr³]octreotide were performed to study binding and uptake of [¹²⁵I-Tyr³]octreotide by lymphoid cell lines (JY, TMM, APD) and primary cells derived from a B-cell-derived chronic lymphatic leukemia. **Results:** A selective expression of sst₂ and sst₃ messenger RNA (mRNA) was demonstrated. By quantitative RT-PCR, expression levels of sst₂ and sst₃ mRNA were relatively low. Autoradiography studies revealed low binding of [¹²⁵I-Tyr³]octreotide, whereas immunoreactivity could not be detected for sst₂ and sst₃ by immunohistochemistry. On the lymphoid cell lines only low numbers of high-affinity SS binding sites were found. In vitro, uptake of [¹²⁵I-Tyr³]octreotide by these cells was also very low. **Conclusion:** On the basis of our findings, we conclude that lymphomas do not appear to be candidates for radiotherapy using radionuclide-labeled SS analogs. However, lymphomas are highly radiosensitive tumors and further clinical studies should be performed to evaluate whether the low receptor density is sufficient for targeting treatment in these tumors.

Key Words: lymphoma; radiotherapy; somatostatin receptor; autoradiography; internalization

J Nucl Med 2004; 45:8–16

The actions of somatostatin (SS), a 14-amino-acid neuropeptide, are mediated through G-protein-coupled 7-transmembrane receptors. These receptors are named SS receptors (sst) and, until now, 5 different subtypes have been cloned, sst₁₋₅ (1). Throughout the human body, SS has a predominant inhibitory effect, especially with regard to the release of mediators, such as hormones (2). Several studies have shown SS to have antiproliferative (3) and antiangiogenic (4) effects. Apart from the physiologic expression of sst in normal tissues, sst are upregulated in several human malignancies (5). Sst have been demonstrated in most neuroendocrine neoplasms (6), but also in tumors that originate from the central nervous system, breast, and lung (7). After in vitro detection of sst expression in human tumors, peptide receptor scintigraphy using radionuclide-labeled SS analogs was introduced for tumor imaging in diagnosis. Sst-positive neuroendocrine tumors and their metastases could be visualized by scintigraphy after intravenous administration of radionuclide-labeled analogs of SS (8). Moreover, successful treatment of neuroendocrine tumors using radionuclide-labeled SS analogs has been described as well (9). After successful imaging of neuroendocrine tumors, it was demonstrated in patients that also malignant lymphomas could be visualized in vivo with sst scintigraphy (10). However, sensitivity of imaging was found to differ in several studies (11,12) and it was suggested that tumor size was crucial to allow detection (11). In addition, sensitivity to visualize Hodgkin's lymphomas was substantially higher than that for non-Hodgkin's lymphomas (11,13). On the basis of positive sst scintigraphy of lymphoma tissues and their successful implication in treatment of neuroendocrine tumors, it is hypothesized that β -emitting SS analogs may play a future role in radiotherapy of lymphomas as well (14). However, until now, little

Received Feb. 20, 2003; revision accepted Sep. 25, 2003.

For correspondence or reprints contact: Martin P. van Hagen, MD, PhD, Department of Internal Medicine, Room D 443, Erasmus Medical Center, Dr Molewaterplein 50, 3015 GE Rotterdam, The Netherlands.
E-mail: p.m.vanhagen@erasmusmc.nl

was known about both receptor subtype expression and receptor density of the sst in lymphoma tissues. Both aspects are very important with respect to the possible future application of sst-targeting radiotherapy. Moreover, lymphomas of several patients are not visualized by sst scintigraphy (15,16). Therefore, the question was addressed whether this was due to a relatively low receptor density or to absent or differential sst subtype expression. In this study, the expression of messenger RNAs (mRNAs) encoding the 5 different sst subtypes was investigated in a series of human lymphomas. Sst mRNA expression levels were measured quantitatively, using quantitative polymerase chain reaction (Q-PCR) and compared with sst mRNA levels in growth hormone (GH)-secreting pituitary adenomas, which express high levels of sst mRNA. In a previous study it was shown that no SS mRNA itself was expressed in normal cells and tissues of the human immune system. However, expression of the mRNA encoding cortistatin (CST) (17), a SS-like peptide, was detected. CST is also capable of binding with high affinity to all 5 sst (18). In this study we investigated the mRNA expression of both SS and CST in lymphomas. To answer the question of whether radionuclide-labeled SS analogs may also be used in the treatment of lymphomas, next to the Q-PCR studies, receptor–ligand internalization and membrane binding studies were performed with a SS-like radiolabeled compound, [125 I-Tyr 3]octreotide, to evaluate internalization of SS-coupled radioactivity by different lymphoid cell lines as a model for binding and internalization of the receptors expressed in the lymphoma tissues. By autoradiography, specific binding of [125 I-Tyr 3]octreotide, which binds with high affinity to sst $_2$, was evaluated and quantified in a series of lymphoma sections. The expression of sst $_2$ and sst $_3$ was also studied by immunohistochemistry. Finally, to exclude possible mutations in the sst $_2$ receptor, DNA from 4 lymphomas was analyzed by sequencing.

MATERIALS AND METHODS

Tissues

Orbital lymphomas ($n = 6$), Hodgkin's lymphomas ($n = 2$), and non-Hodgkin's lymphomas from the neck region ($n = 2$) were collected during diagnostic biopsies and surgical intervention, quickly frozen in liquid nitrogen, and stored at -80°C until use or selected on the presence of archived frozen material. Histopathologic classification of the tissues studied is shown in Table 1. The 2 Hodgkin's lymphomas from the neck region were classified according to the Ann Arbor Classification and the 2 non-Hodgkin's lymphomas from the neck region were classified according to The National Cancer Institute Working Formulation. The tissues were numbered to ensure anonymity of the patients. Informed consent was obtained from all patients involved.

PCR Studies

Reverse transcriptase PCR (RT-PCR) was performed as described (19). Briefly, poly(A) $^{+}$ mRNA was isolated using Dynabeads Oligo(dT) $_{25}$ (DynaL AS) from malignant lymphoma samples. Complementary DNA (cDNA) was synthesized using the poly(A) $^{+}$ mRNA, which was eluted from the beads in 40 μL H $_2$ O for 10 min at 65°C , using Oligo(dT) $_{12-18}$ Primer (Life Technologies). One-twentieth of the cDNA library was used for each amplification by PCR using primer sets specific for human SS, sst $_{1-5}$, and hypoxanthine-guanine phosphoribosyltransferase (HPRT) as a control (Table 2). As positive controls for SS, CST, and HPRT, cDNA of human brain RNA (Invitrogen) was used. As positive controls for sst $_{1-5}$, DNA from a B lymphoblastoid cell line (BLCL)-BSM cell line (an Epstein-Barr virus-transformed B-cell line) was used. The primer set we used for the detection of CST mRNA was adapted from Ejekskär et al. (20). The PCR was performed in a DNA thermal cycler with heated lid (Applied Biosystems). After an initial denaturation at 94°C for 5 min, the samples were subjected to 40 cycles of denaturation at 94°C for 1 min, annealing for 2 min at 60°C , and extension for 1 min at 72°C . After a final extension for 10 min at 72°C , 10- μL aliquots of the resulting PCR products were analyzed by electrophoresis on 1.5% agarose gels stained with ethidium bromide. The identity of the products was confirmed by direct sequencing using an ABI Prism

TABLE 1
Histopathologic Classification of Different Tissues and Their Receptor Subtype Expression

Tissue		mRNA						
No.	Classification	sst $_1$	sst $_2$	sst $_3$	sst $_4$	sst $_5$	SS	CST
Orbital region								
1	ML-MALT	—	+	+	—	—	—	+
2	Follicular center lymphoma	—	+	+	—	—	—	+
3	Mantle cell lymphoma	—	+	+	—	—	—	+
4	Diffuse large B-cell lymphoma	—	+	+	—	—	—	+
5	Mantle cell lymphoma	—	+	+	—	—	—	+
6	Follicular center lymphoma	—	+	+	—	—	—	+
Neck region								
7	Hodgkin's lymphoma, stage I	—	+	—	—	—	—	+
8	Hodgkin's lymphoma, stage II	—	+	—	—	—	—	+
9	Low-grade non-Hodgkin's lymphoma	—	+	—	—	—	—	+
10	Intermediate-grade non-Hodgkin's lymphoma	—	+	—	—	—	—	+

ML-MALT = extranodal marginal zone B-cell lymphoma (where MALT = mucosa-associated lymphoid tissue).

TABLE 2
Primers Used for RT-PCR

Primer	Sequence (5'→3')	Size of PCR product (bp)
sst ₁ forward	ATGGTGGCCCTCAAGGCCGG	318
sst ₁ reverse	CGCGGTGGCGTAATAGTCAA	
sst ₂ forward	GCCAAGATGAAGACCATCAC	414
sst ₂ reverse	GATGAACCTGTGTACCAAGC	
sst ₃ forward	TCATCTGCCTCTGTACCTG	221
sst ₃ reverse	GAGCCCAAAGAAGGCAGGCT	
sst ₄ forward	ATCTTCGCAGACACCAGACC	323
sst ₄ reverse	ATCAAGGCTGGTCACGACGA	
sst ₅ forward	CCGTCTTCATCATCTACACGG	223
sst ₅ reverse	GGCCAGGTTGACGATGTTGA	
HPRT forward	CAGGACTGAACGTCTTGCTC	413
HPRT reverse	CAATCCAACAAAGTCTGGC	
SS forward	GATGCTGTCTGCCGCTCCAG	349
SS reverse	ACAGGATGTGAAAGTCTTCCA	
CST forward	GCAAATTCGCTCTAAACACAGGA	173
CST reverse	TTGGGAAGGAGGAGGAAAGAT	

bp = base pairs.

3100 Genetic Analyzer (Applied Biosystems) according to the manufacturer's protocol.

To quantify expression of sst mRNAs, a Q-PCR was performed by the TaqMan Gold nuclease assay (Perkin Elmer Corp.) and the ABI PRISM 7700 sequence Detection System (Perkin Elmer) for real-time amplifications, according to the manufacturer's protocol. Q-PCR was performed for sst₂ and sst₃ only, because no expression of the other sst subtypes could be detected in the tissues and cells we investigated by RT-PCR. The primer sequences used are summarized in Table 3. In each experiment, standard curves for each primer set were included. Known amounts of genomic DNA containing sst_{2A} and sst₃ or dilutions of a pool of HPRT-containing cDNAs were amplified (in duplicate or triplicate) together with the unknown cDNA samples. A standard curve was constructed by plotting the threshold-cycle (Ct) versus the logarithm of the starting quantity. With these standard curves and the measured Ct of the unknown cDNA samples, the starting amounts in the cDNA samples were determined in duplicate or triplicate. To correct for differences in the efficiency of RNA isolation and cDNA synthesis, the amounts of sst_{2A} and sst₃ were divided by the amount of HPRT in a given cDNA sample. Since the absolute copy number of HPRT templates in the control cDNAs used for the HPRT standard curve is unknown, the starting amounts are given in arbitrary units. Reaction conditions were optimized until the SD of duplicate determinations of the Ct of standard curve samples was <3%. A linear correlation existed between the logarithm of the starting amount of the template and the Ct in the range of >300,000 copies down to approximately 30 copies. Below 30 copies, duplicate measurements displayed less accuracy due to more delays or failures of amplification. Above 30 copies starting amount, the SD of the copy number calculated by means of the standard curve ranged from 5% to 20%. The data of Q-PCR are therefore presented as the ratio of sst₂ or sst₃ over HPRT, which makes it possible to compare the different samples. Because the absolute copy number of HPRT templates in the control cDNAs for HPRT is unknown, final data are presented as arbitrary units.

Internalization Studies

Internalization experiments were performed as described in detail (21) using [¹²⁵I-Tyr³]octreotide (kindly provided by Dr. Wout Breeman, Department of Nuclear Medicine, Erasmus Medical Center, Rotterdam, The Netherlands) (22). In short, 10⁶ cells were seeded per well in 24-well plates (Costar Corning) and incubated with approximately 400,000 cpm/mL [¹²⁵I-Tyr³]octreotide with or without an excess of unlabeled peptide. After different periods of incubation (30, 60, 120 min), cell-surface-bound radioligand was removed with a 1-mL acid wash for 10 min (21). Internalized radioligand was measured as acid-resistant counts in pellets of the acid-washed cells. The cell lines we studied included 1 myeloid leukemic cell line (TMM), a lymphoid B-cell line (JY), an EBV-transfected APD cell line, and EBV-immortalized primary B-cells from a patient with a B-cell-derived chronic lymphatic leukemia (B-CLL). The differentiation state (marker pattern) of the cell lines we used was comparable with that of solid lymphomas or leukemias. To our knowledge, no specific orbit lymphoma cell lines were reported in the literature. As a positive control for sst₂-mediated internalization, stably sst₂-transfected CC531 colon adenocarcinoma cells were used (CC2B). CC531 cells were established from an adenocarcinoma and maintained by trypsinization and serial passage in culture medium (23). The human sst₂ cDNA in pBluescript was a kind gift from Dr. Graeme I. Bell (Howard Hughes Medical Institute). This sst₂ cDNA was excised from pBluescript and inserted into the *Nhe* I and *Sal* I cloning sites of the retroviral vector pCI-neo (Promega Corp.). This vector was used to generate the CC2B cells.

Binding Studies

Membrane isolation and binding studies were performed as described (24) on the above indicated cells. In short, membrane preparations (corresponding to 30–50 µg of protein) were incubated in a total volume of 100 µL at room temperature for 60 min with increasing concentrations of [¹²⁵I-Tyr³]octreotide without and with an excess (1 µmol/L) of unlabeled octreotide in *N*-(2-hydroxyethyl)piperazine-*N'*-(2-ethanesulfonic acid) (HEPES) buffer (10 mmol/L HEPES, 5 mmol/L MgCl₂, and 0.02 g/L bacitracin, pH 7.6) containing 0.2% bovine serum albumin (BSA). After the incubation, 1 mL ice-cold HEPES buffer was added to the reaction mixture, and membrane-bound radioactivity was separated from unbound radioactivity by centrifugation during 2 min at 14,000 rpm in an Eppendorf microcentrifuge. The remaining

TABLE 3
Primers Used for Q-PCR

Primer	Sequence (5'→3')
sst ₂ forward	-ATGCCAAGATGAAGACCATCAC-
sst ₂ reverse	-TGAAGTATGATGCCATCCA-
sst ₂ probe	-FAM-TGGCTCTGGTCCACTGGCCCTTTG-TAMRA-
sst ₃ forward	CTGGGTAACTCGCTGGTCATCTA-
sst ₃ reverse	AGCGCCAGGTTGAGGATGTA-
sst ₃ probe	-FAM-CGGCCAGCCCTTCAGTCACCAAC-TAMRA
HPRT forward	-TGCTTTCCTTGCTCAGGCAGTAT-
HPRT reverse	-TCAAATCCAACAAAGTCTGGCTTATATC-
HPRT probe	-FAM-CAAGCTTGGACCTTGACCATCTTTGGA-TAMRA-

FAM = carboxyfluorescein; TAMRA = carboxytetramethylrhodamine.

pellet was washed twice in ice-cold HEPES buffer, and the pellet was counted in a γ -counter (1470 Wizard; Wallac). Specific binding was taken to be the total binding minus binding in the presence of 1 μ mol/L unlabeled octreotide.

Binding of [125 I-Tyr 3]octreotide to sst in the malignant lymphoma tissues was investigated by autoradiography on unfixed cryosections. Malignant lymphoma biopsies were taken and immediately frozen, and small parts were embedded in TissueTek (Miles Inc.) and processed for cryosectioning. Twenty-micrometer-thick sections were mounted on gelatin-coated glass slides and stored at -80°C for 3 d to improve adhesion of the tissue sections to the slides. Autoradiography was performed on cryostat sections of malignant lymphoma tissue and sections of neuroendocrine tumors, serving as a positive control for binding to sst $_2$ specifically, as described (25). Binding of [125 I-Tyr 3]octreotide was displaced by an excess of unlabeled octreotide to show specificity of binding. The number of pixels was quantified automatically using a Phosphor Imager (Amersham Biosciences). Specific binding was defined by $>50\%$ displacement of the autoradiographic signal by excess unlabeled octreotide.

Immunohistochemistry was performed on 5- μ m-thick sections cut on a cryostat (Jung CM3000; Leica) as described in detail (26). Sections were incubated overnight at 4°C with sst $_2$ (Biotrend) and sst $_3$ (Biotrend) antibodies, using 1:2,000 and 1:3,000 dilutions in phosphate-buffered saline (PBS) + 5% BSA, respectively. A standard streptavidin-biotinylated-horseradish peroxidase complex (ABC kit; Biogenex) was used according to the manufacturer's protocol. Finally, sections were developed with diaminobenzidine and mounted. Paraffin-embedded sections (5 μ m) were deparaffinized, rehydrated, exposed to microwave heating (in citric acid buffer, pH 6.0) at 100°C for 15 min, and rinsed in tap water followed by PBS. Subsequent steps were performed as in the protocol for frozen sections. The antibodies were used at dilutions of 1:2,000 in PBS + 5% BSA and sections were incubated overnight at 4°C . Human pancreatic tissue served as a positive control for expression of sst. Finally, to detect possible mutations in the sst $_2$ gene, purified PCR products were sequenced on an ABI Prism 310 Genetic Analyzer, using a BigDye Terminator Cycle Sequencing Ready Reaction DNA sequencing kit (Applied Biosystems).

RESULTS

Results by RT-PCR are summarized in Table 1. In the 2 Hodgkin's and 2 non-Hodgkin's lymphomas from the neck region, only expression of sst $_2$ mRNA could be detected. In all orbital lymphomas, sst $_2$ and sst $_3$ mRNA was demonstrated. SS mRNA could not be detected in any of the tissues tested. However, CST mRNA was expressed in all tissue samples. Results of the Q-PCR are shown in Table 4. By Q-PCR, expression levels of sst $_2$ and sst $_3$ mRNA were studied. Sst $_2$ mRNA levels in the lymphoma tissues were compared with the expression of sst $_2$ mRNA in GH-secreting pituitary adenomas, which express high levels of sst $_2$ mRNA. As shown, the expression levels of sst $_2$ and sst $_3$ mRNA in the lymphoma tissues are relatively low, the highest relative expression of sst $_2$ mRNA in the lymphomas being 208 copies when adjusted for HPRT. When compared with GH-secreting pituitary adenomas, these sst $_2$ mRNA levels were 6- to 200-fold lower in the malignant lymphoma-

TABLE 4
Quantitative Expression of sst mRNA in Lymphoma Tissues Compared with sst mRNA Expression in 2 GH-Secreting Pituitary Adenomas

Lymphoma no.	sst $_2$ /HPRT*	sst $_3$ /HPRT	GH-secreting pituitary adenoma no.	sst $_2$ /HPRT	sst $_3$ /HPRT
8	208	†	1	1,714	1,260
1	115	‡	2	1,020	2,140
10	65	†			
7	32	†			
9	30	†			
5	28	26			
2	13	‡			
6	13	‡			
4	8	9			
3	6	‡			

*Values represent arbitrary units, generated to a standard curve. Values are presented as ratio of number of copies of sst over number of copies of HPRT, both relative to a standard curve.

†Quantitative RT-PCR was not performed, as no expression of sst $_1$ or sst $_3$ was found by RT-PCR.

‡Expression was below detection limit of quantitative RT-PCR.

mas. Although we found positive signals for sst $_2$ and sst $_3$ mRNA in the different tissues using RT-PCR, we showed by Q-PCR that these bands represent only very low expression levels of sst $_2$. Sst $_3$ mRNA expression levels were very low as well, or even below the detection limit in most tissues tested.

Autoradiographic studies were performed to investigate and quantify binding of the sst $_2$ -specific agonist, [125 I-Tyr 3]octreotide, to sst $_2$ in malignant lymphomas. Rat brain and a human GH-secreting pituitary adenoma served as positive controls. Both control samples showed high specific binding of [125 I-Tyr 3]octreotide. A series of 6 orbital lymphomas (numbers 1–6) were incubated with [125 I-Tyr 3]octreotide without or with unlabeled octreotide. Specific binding of [125 I-Tyr 3]octreotide was detected in all orbital lymphomas. However, compared with rat brain and a GH-secreting pituitary adenoma, total binding of [125 I-Tyr 3]octreotide was much lower in the malignant lymphomas, as shown in Figure 1. The binding of [125 I-Tyr 3]octreotide was quantified using a Phosphor Imager. The intensity of black spots, which represent binding of [125 I-Tyr 3]octreotide to sst $_2$, was set at 100% in the GH-secreting pituitary adenoma, and the intensity in the lymphomas was calculated relative to the intensity in the positive control, as shown in Table 5. All malignant lymphomas studied have very low total binding, with the highest being $<14\%$ of the binding to the GH-secreting pituitary adenoma and $<20\%$ of the binding in rat brain cortex, indicating a very low expression of the sst $_2$ receptors in these tissues. These findings correspond to the relatively low expression levels of sst $_2$ mRNA found by Q-PCR.

By immunohistochemistry using sst $_2$ - and sst $_3$ -specific polyclonal antibodies, an attempt was made to visualize sst $_2$

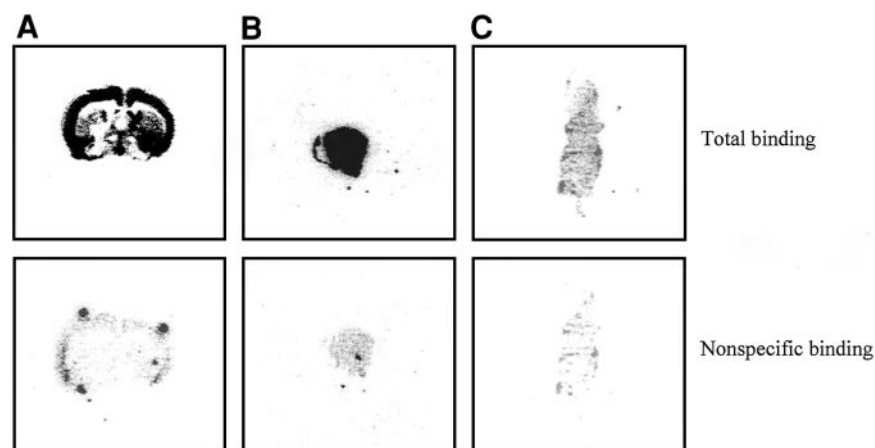


FIGURE 1. Autoradiography experiments on lymphomas. (Top) Binding of [125 I-Tyr 3]-octreotide, represented by black spots, to rat brain (A), GH-producing tumor (B), both used as positive controls, and example of 1 lymphoma studied (C), lymphoma no. 6. (Bottom) Binding of [125 I-Tyr 3]octreotide is displaced by excess unlabeled octreotide.

and ss_{t3} in malignant lymphoma tissue. Human pancreas served as a positive control. Sst_2 and ss_{t3} immunoreactivity was clearly detected in the pancreatic islets with a pattern of expression as described (6). This immunostaining could be completely abolished by preabsorption of the respective antibodies with 100 nmol/L of the peptide antigen (data not shown). However, under the conditions used, we were unable to detect immunoreactivity for ss_{t2} and ss_{t3} in the different lymphomas. To further evaluate this conclusion, membrane binding and internalization studies were performed to evaluate the amount of radiolabeled octreotide bound and internalized by the ss_{t2} on the cell membranes. For these experiments, we used B-lymphoid and myeloid cell lines as a model for cells of malignant lymphoma tissues. As a positive control, the stably ss_{t2} -transfected colon adenocarcinoma cells (CC2B) were used. Q-PCR was performed to investigate the ss_{t2} mRNA expression levels in the cell lines we used. The data are summarized in Table 6, which represents the relative amount of ss_{t2} mRNA expres-

sion in different cell lines, calculated relative to a standard curve, generated from a Jurkat cell line and given in arbitrary units as the relative amount of ss_{t2} mRNA per 750,000 cells isolated. A CC531 cell line was used as the untransfected negative control

Although all cell lines expressed ss_{t2} mRNA, expression levels were relatively low compared with that of the stably ss_{t2} -expressing CC2B cell line. To investigate the expression levels of the ss_{t2} protein in the different cell lines, membrane binding studies were performed. The results are shown in Figure 2. All cells investigated showed high-affinity binding sites for SS; however, the number of receptors was found to be low. To investigate the extent to which these receptors are able to internalize the radionuclide-coupled SS analog, internalization experiments were performed using [125 I-Tyr 3]octreotide.

As shown in Figure 3, the CC2B cells internalized significantly higher amounts of [125 I-Tyr 3]octreotide than the JY, TMM, and APD cell lines. No internalization could be detected in the primary B-CLL cells.

Finally, DNA obtained from lymphoma tissues was used for sequencing to detect possible mutations in the DNA sequence in the ss_{t2} coding region in malignant lymphomas. Four orbital lymphomas were studied (numbers 1, 3, 4, and 6). No mutations could be detected (data not shown).

TABLE 5
Autoradiography Experiments on Lymphoma Tissues

Tissue	% binding
GH-producing tumor	100
Rat brain	72
Lymphoma no.	
5	13.8
1	13.7
2	9.5
6	7.7
3	7.1
4	7.0

Binding percentages of [125 I-Tyr 3]octreotide in lymphoma tissues are measured using Phosphor Imager, in which number of pixels was quantified. Pixels represent binding of [125 I-Tyr 3]octreotide to tissue. Specific binding of [125 I-Tyr 3]octreotide to GH-producing tumor was set at 100% and amount of binding of radiolabeled compound to different lymphoma tissues is presented relative to that of GH-producing tumor.

TABLE 6
Quantitative Expression of ss_{t2} in Different B- and Myeloid Cell Lines

Cells	ss_{t2} per 750,000 cells
APD	11,770
JY	11,230
TMM	8,155
B-CLL	490
CC531	*
CC2B	72,000

*CC531 cell line was used as an untransfected negative control.

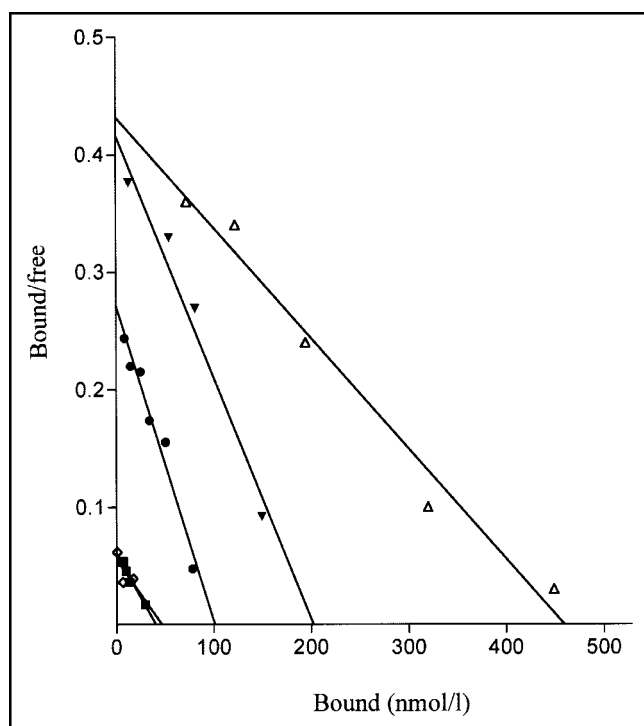


FIGURE 2. Membrane binding studies. Scatchard analysis of [125 I]-Tyr³]octreotide binding on human B and myeloid cell lines: \diamond , B-CLL (dissociation constant [K_d] = 0.8 nmol/L, n = 50 fmol/mg); \blacksquare , APD cell line (K_d = 0.7 nmol/L, n = 40 fmol/mg); \bullet , TMM cell line (K_d = 0.4 nmol/L, n = 100 fmol/mg); \blacktriangledown , JY cell line (K_d = 0.4 nmol/L, n = 195 fmol/mg); \triangle , CC2B cell line (K_d = 0.8 nmol/L, n = 460 fmol/mg).

DISCUSSION

Previously, it had been demonstrated by sst scintigraphy that malignant lymphomas express sst (10,27). The sensitivity of sst scintigraphy for Hodgkin's disease lies around 95%–100% (15,16). The sensitivity for non-Hodgkin's lymphomas is around 80% (15). It was shown that uptake of

[111 In-DTPA⁰]octreotide in lymphomas was lower compared with the uptake in neuroendocrine tumors (28,29). Because lymphomas of several patients with malignant lymphoma cannot be visualized by sst scintigraphy, we addressed the question of what the cause of this nonvisualization might be. In addition, our studies addressed the question of whether patients with malignant lymphomas might be candidates for radionuclide-labeled SS analog therapy.

In this study, we investigated the expression of the different sst in a series of malignant lymphomas, using both RT-PCR and Q-PCR. By RT-PCR, in 2 Hodgkin's and 2 non-Hodgkin's lymphomas from the neck region, expression of sst₂ mRNA was detected, whereas the 6 lymphomas originating from the orbital region expressed both sst₂ and sst₃ mRNA. Until now, only a few studies have demonstrated sst in lymphoma tissues using autoradiography (10,27,30), reporting a differential sst subtype expression in malignant lymphoma tissue. In one study, expression of sst₂ mRNA was detected in one Hodgkin's lymphoma and one non-Hodgkin's lymphoma, whereas one non-Hodgkin's lymphoma expressed both sst₁ and sst₃ mRNA (27). Another study showed that extragastric MALT-type lymphomas (where MALT = mucosa-associated lymphoid tissue) expressed sst₂ mRNA, whereas intra-gastric MALT-type lymphomas expressed sst₃ and sst₄ mRNA but not sst₂ mRNA (30). In our previous studies, we were unable to detect expression of sst₄ in the human immune system and in human malignancies.

The expression pattern of the sst subtypes was further studied by Q-PCR, and results were compared with sst expression in 2 GH-secreting pituitary adenomas expressing high levels of sst. We found relatively low levels of sst₂ and sst₃ mRNA expression in all lymphomas studied compared with that of the pituitary adenomas. Autoradiography and immunohistochemistry further supported these findings. By autoradiography, very low specific binding of [125 I]-

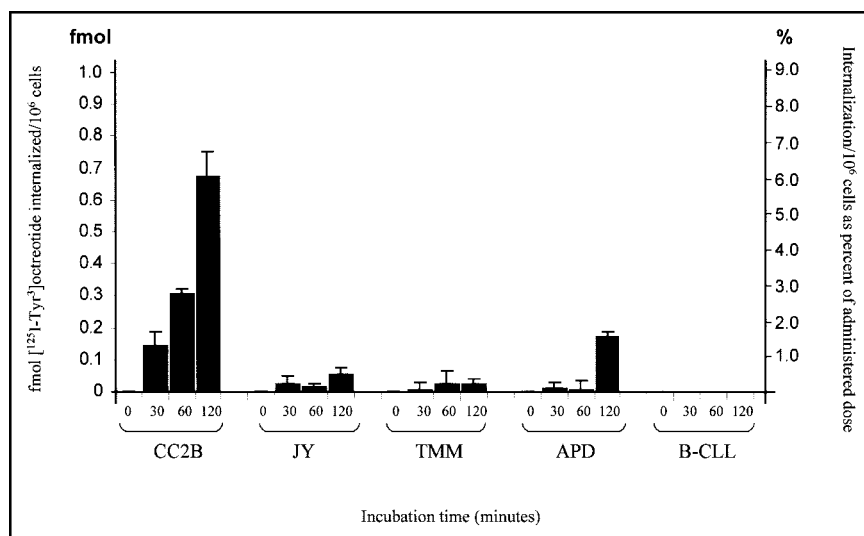


FIGURE 3. Internalization experiment using CC2B, JY, TMM, APD, and B-CLL cells. Cells were incubated either with [125 I]-Tyr³]octreotide alone or with [125 I]-Tyr³]octreotide and excess of unlabeled octreotide (1 μ mol/L) for 30, 60, and 120 min, respectively. At each time point, internalization was measured. Results are presented as amount of radiolabeled compound internalized by cell in fmol/ 10^6 cells and as degree of internalization for 10^6 cells as percentage of administered dose.

Tyr³]octreotide was demonstrated and by immunohistochemistry sst₂ or sst₃ could not be visualized. This low or absent specific binding can be explained by low receptor levels in these tissues, in agreement with the low sst mRNA levels encoding the receptor proteins found by Q-PCR. It should be taken into consideration that sst₂-expressing inflammatory cells infiltrating the lymphomas may account for the sst₂ expression levels detected by Q-PCR. However, we found the infiltration rate to be <5%. Therefore, the contribution of potential infiltrating cells to sst₂ mRNA levels we detected will be very small. Moreover, these infiltrating cells, which may express sst₂, will not influence the results and interpretation of the Q-PCR, as the outcome was a very low expression of sst₂ mRNA in lymphoma tissues. The variable positive results obtained by sst scintigraphy in malignant lymphomas in previous studies (15,16,29) have been attributed to small lesion sizes (11,16). However, these negative findings might also be explained by very low expression of the receptors on the cell membranes, as demonstrated in our study. To study the internalization of radionuclide-coupled SS analogs, we used several cell lines and one sample of primary B-CLL cells because fresh lymphoma cells were difficult to obtain. Scatchard analysis of these cell lines and B-CLL cells revealed that all cells used showed relatively low levels of high-affinity binding sites and very low internalization, which is in agreement with the low number of SS binding sites. The sst₂-expressing CC2B cells internalized significantly higher amounts of the radiolabeled compound. An explanation for the relatively low sst levels and low internalization of radiolabeled SS analogs may be endogenous SS production as has been demonstrated in pheochromocytomas (31). Endogenous SS production may facilitate internalization of the sst₂ in an autocrine fashion (31); thus, a lower uptake of radiolabeled SS analogs may be expected in SS-expressing tissues. We evaluated expression of SS mRNA in lymphoma tissues to find an alternative explanation for the low uptake of radionuclide-labeled SS analogs by these cells. No SS mRNA in any of the lymphoma tissues studied was detected, however. Recently, we demonstrated that the SS-like peptide CST is expressed in normal cells of the human immune system (17). CST might act as alternative ligand to sst, rather than SS itself, because of its high binding affinity to all 5 sst (18). Therefore, we also investigated the expression of CST mRNA in the lymphomas. We detected expression in all samples tested instead of the expression of SS mRNA. Although, until now, we could not detect the protein CST, it might be suggested on the basis of the expression of CST mRNA that CST can also facilitate internalization of the sst₂ on the cell membrane and cause a lower uptake of radioactively labeled SS analogs as well. Further studies should be performed to elucidate this issue.

To exclude the possibility that mutations in the coding region of the sst₂ gene might be responsible for low-efficiency internalization, DNA from 4 malignant lymphomas was sequenced. No mutations in the sst₂ coding region could

be detected, ruling out that the low internalization rate could be caused by a defect in the receptor. Based on our findings of low sst numbers, low binding, and internalization, lymphomas appear not to be good candidates for radiotherapy using radiolabeled SS analogs. However, recently, advances have been made in gene transfer of sst in defined cancer cells (32–34). It has been demonstrated that the induction of sst₂ in both primary and metastatic pancreatic cancer models results in a significant antitumor effect characterized by an increase of apoptosis and an inhibition of cell proliferation (33). In rat colon carcinoma cell lines, induction of sst₂ also led to an induced antitumor effect with peptide receptor radionuclide therapy (34). In the sst₂-transfected CC2B cells, we indeed found very effective internalization of the radionuclide-coupled SS analog. This finding might be promising with respect to a possible combination of sst gene therapy and SS analog radiotherapy in, for example, lymphoma tissues. Further studies must be performed to elucidate this interesting topic as, in solid tumors, it has been demonstrated that gene therapy using either retroviral or adenoviral vectors with the p53 gene in non-small cell lung cancers resulted in tumor regression or stabilization in most patients (35).

In summary, we investigated the expression of sst, both qualitatively and quantitatively, in different malignant lymphomas, as well as the expression of the natural ligand SS, to answer the question of whether SS or its analogs might play a future role in radiotherapy treatment of these diseases. We demonstrated very low expression levels of sst mRNA and, subsequently, low or absent specific binding to these tissues in our autoradiography and immunohistochemistry experiments. Although previous studies showed expression of sst in different lymphoma tissues (10), it was also clearly demonstrated that lesions were not detected using the sst scintigraphy in all patients (15,29). We hypothesize that these negative results might be due to a very low expression of the sst in malignant lymphomas. In the literature, it was hypothesized that SS or one of its analogs might play a future role in treatment of malignant lymphomas, either as “cold” peptides (36) or as β -emitting radionuclide-coupled peptides (14). In our cell line models, we demonstrated that, despite expression of the sst₂, internalization capacity is very low but could be enhanced by overexpression of sst₂. These data suggest that lymphomas in vivo might not be a target for radiotherapy with SS or its analogs. However, malignant lymphomas are the human tumors that are most sensitive to radiation (37). In contrast, neuroendocrine tumors, such as carcinoids and gastrinomas, are considered to be rather radioresistant. However, successful tumor shrinkage has been reported in neuroendocrine tumors after ¹⁷⁷Lu-DOTA-Tyr³-octreotate administration (38). On the other hand, previous studies demonstrated clearly that the internalization of radionuclide-labeled SS analogs in cell models was time dependent and, thus, increased over time (21,39). In our internalization studies, we also found an increased uptake over time. Therefore, it may

be hypothesized that the use of longer incubation periods may enhance the uptake of radionuclide-labeled SS analogs in lymphoma patients and, thus, the utility of therapy with these analogs. On the other hand, longer incubation periods with radionuclide-labeled SS analogs may cause damage to other sst-expressing organs, such as kidney, spleen, and bone marrow (40). This is a major disadvantage, because of the importance of these organs in the human organism. Therefore, caution should be taken when considering the use of longer incubation periods with radionuclide-labeled SS analogs to treat lymphoma patients. Future clinical trials will show whether, in human lymphomas, the higher radiosensitivity will be sufficient to compensate for low sst numbers and low efficiency of internalization compared with that of neuroendocrine tumors.

CONCLUSION

In this study, we demonstrated that malignant lymphomas expressed relatively low levels of sst, both at mRNA and protein levels. In cell line models, low uptake of radioactively labeled SS analogs was found. Low uptake was not due to mutations in the *sst₂* gene. Therefore, we conclude that the low uptake is based on low receptor numbers and, thus, malignant lymphomas may not be targets for therapy using radionuclide-labeled SS analogs, as has been suggested previously. However, it should be taken into consideration that lymphomas are highly radiosensitive tumors and relative low uptake might still be efficient in reducing the number of tumor cells. This should be further evaluated in clinical conditions.

ACKNOWLEDGMENTS

We cordially acknowledge Dr. Wout A. Breeman (Department of Nuclear Medicine, Erasmus Medical Center, Rotterdam, The Netherlands) for his contribution to this work and Dr. Rebecca Croxen (Eye Hospital Rotterdam, The Netherlands) for reviewing the English of this manuscript. This work was supported by a grant (903-43-092) from the Dutch Organization for Scientific Research.

REFERENCES

- Patel YC. Somatostatin and its receptor family. *Front Neuroendocrinol*. 1999; 20:157–198.
- Brazeau P. Somatostatin: a peptide with unexpected physiologic activities. *Am J Med*. 1986;81:8–13.
- Kvols LK, Moertel CG, O'Connell MJ, Schutt AJ, Rubin J, Hahn RG. Treatment of the malignant carcinoid syndrome: evaluation of a long-acting somatostatin analogue. *N Engl J Med*. 1986;315:663–666.
- Patel PC, Barrie R, Hill N, Landeck S, Kurozawa D, Woltering EA. Postreceptor signal transduction mechanisms involved in octreotide-induced inhibition of angiogenesis. *Surgery*. 1994;116:1148–1152.
- Hoffland LJ, Lamberts SW. Somatostatin receptor subtype expression in human tumors. *Ann Oncol*. 2001;12:S31–S36.
- Kulaksiz H, Eissele R, Rossler D, et al. Identification of somatostatin receptor subtypes 1, 2A, 3, and 5 in neuroendocrine tumours with subtype specific antibodies. *Gut*. 2002;50:52–60.
- Reubi JC, Krenning E, Lamberts SW, Kvols L. In vitro detection of somatostatin receptors in human tumors. *Digestion*. 1993;54:76–83.
- Krenning EP, Bakker WH, Breeman WA, et al. Localisation of endocrine-related tumours with radioiodinated analogue of somatostatin. *Lancet*. 1989;333:242–244.
- Breeman WA, de Jong M, Kwekkeboom DJ, et al. Somatostatin receptor-mediated imaging and therapy: basic science, current knowledge, limitations and future perspectives. *Eur J Nucl Med*. 2001;28:1421–1429.
- Vanhagen PM, Krenning EP, Reubi JC, et al. Somatostatin analogue scintigraphy of malignant lymphomas. *Br J Haematol*. 1993;83:75–79.
- Lipp RW, Silly H, Ranner G, et al. Radiolabeled octreotide for the demonstration of somatostatin receptors in malignant lymphoma and lymphadenopathy. *J Nucl Med*. 1995;36:13–18.
- Ivancevic V, Worman B, Nauck C, et al. Somatostatin receptor scintigraphy in the staging of lymphomas. *Leuk Lymphoma*. 1997;26:107–114.
- Kwekkeboom D, Krenning EP, de Jong M. Peptide receptor imaging and therapy. *J Nucl Med*. 2000;41:1704–1713.
- Virgolini I, Patri P, Novotny C, et al. Comparative somatostatin receptor scintigraphy using in-111-DOTA-lanreotide and In-111-DOTA-Tyr³-octreotide versus F-18-FDG-PET for evaluation of somatostatin receptor-mediated radionuclide therapy. *Ann Oncol*. 2001;12:S41–S45.
- Limouris GS, Rassidakis A, Kondi-Papithi A, et al. Somatostatin receptor scintigraphy of non-neuroendocrine malignancies with ¹¹¹In-pentetreotide. *Anticancer Res*. 1997;17:1593–1597.
- Lugtenburg PJ, Krenning EP, Valkema R, et al. Somatostatin receptor scintigraphy useful in stage I-II Hodgkin's disease: more extended disease identified. *Br J Haematol*. 2001;112:936–944.
- Dalm VA, van Hagen PM, van Koetsveld PM, et al. Cortistatin rather than somatostatin as a potential endogenous ligand for somatostatin receptors in the human immune system. *J Clin Endocrinol Metab*. 2003;88:270–276.
- Fukusumi S, Kitada C, Takekawa S, et al. Identification and characterization of a novel human cortistatin-like peptide. *Biochem Biophys Res Commun*. 1997; 232:157–163.
- Ferone D, van Hagen PM, van Koetsveld PM, et al. In vitro characterization of somatostatin receptors in the human thymus and effects of somatostatin and octreotide on cultured thymic epithelial cells. *Endocrinology*. 1999;140:373–380.
- Ejsskar K, Abel F, Sjöberg R, Backstrom J, Kogner P, Martinsson T. Fine mapping of the human preproctistatin gene (CORT) to neuroblastoma consensus deletion region 1p36.3→p36.2, but absence of mutations in primary tumors. *Cytogenet Cell Genet*. 2000;89:62–66.
- Hoffland LJ, van Koetsveld PM, Waaijers M, Zuyderwijk J, Breeman WA, Lamberts SW. Internalization of the radioiodinated somatostatin analog [¹²⁵I-Tyr³]octreotide by mouse and human pituitary tumor cells: increase by unlabeled octreotide. *Endocrinology*. 1995;136:3698–3706.
- Bakker WH, Krenning EP, Breeman WA, et al. In vivo use of a radioiodinated somatostatin analogue: dynamics, metabolism, and binding to somatostatin receptor-positive tumors in man. *J Nucl Med*. 1991;32:1184–1189.
- Marquet RL, Westbroek DL, Jeekel J. Interferon treatment of a transplantable rat colon adenocarcinoma: importance of tumor site. *Int J Cancer*. 1984;33:689–692.
- Reubi JC. New specific radioligand for one subpopulation of brain somatostatin receptors. *Life Sci*. 1985;36:1829–1836.
- ten Bokum AM, Hoffland LJ, de Jong G, et al. Immunohistochemical localization of somatostatin receptor *sst2A* in sarcoid granulomas. *Eur J Clin Invest*. 1999; 29:630–636.
- Hoffland LJ, Liu Q, Van Koetsveld PM, et al. Immunohistochemical detection of somatostatin receptor subtypes *sst1* and *sst2A* in human somatostatin receptor positive tumors. *J Clin Endocrinol Metab*. 1999;84:775–780.
- Reubi JC, Schaer JC, Waser B, Mengod G. Expression and localization of somatostatin receptor *SSTR1*, *SSTR2*, and *SSTR3* messenger RNAs in primary human tumors using in situ hybridization. *Cancer Res*. 1994;54:3455–3459.
- Leners N, Jamar F, Fiasse R, Ferrant A, Pauwels S. Indium-111-pentetreotide uptake in endocrine tumors and lymphoma. *J Nucl Med*. 1996;37:916–922.
- Sarda L, Duet M, Zini JM, et al. Indium-111 pentetreotide scintigraphy in malignant lymphomas. *Eur J Nucl Med*. 1995;22:1105–1109.
- Raderer M, Valencak J, Pfeffel F, et al. Somatostatin receptor expression in primary gastric versus nongastric extranodal B-cell lymphoma of mucosa-associated lymphoid tissue type. *J Natl Cancer Inst*. 1999;91:716–718.
- Reubi JC, Waser B, Liu Q, Laissue JA, Schonbrunn A. Subcellular distribution of somatostatin *sst2A* receptors in human tumors of the nervous and neuroendocrine systems: membranous versus intracellular location. *J Clin Endocrinol Metab*. 2000;85:3882–3891.
- Fisher WE, Wu Y, Amaya F, Berger DH. Somatostatin receptor subtype 2 gene therapy inhibits pancreatic cancer in vitro. *J Surg Res*. 2002;105:58–64.
- Vernejoul F, Faure P, Benali N, et al. Antitumor effect of in vivo somatostatin receptor subtype 2 gene transfer in primary and metastatic pancreatic cancer models. *Cancer Res*. 2002;62:6124–6131.

34. Mearadji A, Breeman W, Hofland L, et al. Somatostatin receptor gene therapy combined with targeted therapy with radiolabeled octreotide: a new treatment for liver metastases. *Ann Surg.* 2002;236:722–728.
35. Giaccone G. Clinical impact of novel treatment strategies. *Oncogene.* 2002;21:6970–6981.
36. O'Brien JP. Somatostatin receptor-based imaging in malignant lymphomas. *J Nucl Med.* 1995;36:19–20.
37. Deacon J, Peckham MJ, Steel GG. The radioresponsiveness of human tumours and the initial slope of the cell survival curve. *Radiother Oncol.* 1984;2:317–323.
38. Kwekkeboom DJ, Bakker WH, Kooij PP, et al. [¹⁷⁷Lu-DOTA⁰Tyr³]octreotate: comparison with [¹¹¹In-DTPA⁰]octreotide in patients. *Eur J Nucl Med.* 2001;28:1319–1325.
39. De Jong M, Bernard BF, De Bruin E, et al. Internalization of radiolabelled [DTPA⁰]octreotide and [DOTA⁰,Tyr³]octreotide: peptides for somatostatin receptor-targeted scintigraphy and radionuclide therapy. *Nucl Med Commun.* 1998;19:283–288.
40. Tiensuu Janson E, Eriksson B, Oberg K, et al. Treatment with high dose [¹¹¹In-DTPA-D-PHE¹]octreotide in patients with neuroendocrine tumors: evaluation of therapeutic and toxic effects. *Acta Oncol.* 1999;38:373–377.



In the article “¹²³I-Hippuran Renal Scintigraphy with Evaluation of Single-Kidney Clearance for Predicting Renal Scarring After Acute Urinary Tract Infection: Comparison with ^{99m}Tc-DMSA Scanning,” by Imperiale et al. (*J Nucl Med.* 2003;44:1755–1760), the fifth author was listed incorrectly because of a copyediting error. The correct name is Daniela Seracini, MD. We regret the error.



The Journal of
NUCLEAR MEDICINE

Somatostatin Receptors in Malignant Lymphomas: Targets for Radiotherapy?

Virgil A.S.H. Dalm, Leo J. Hofland, Cornelia M. Mooy, Marlijn A. Waaijers, Peter M. van Koetsveld, Anton W. Langerak, Frank T.J. Staal, Aart-Jan van der Lely, Steven W.J. Lamberts and Martin P. van Hagen

J Nucl Med. 2004;45:8-16.

This article and updated information are available at:

<http://jnm.snmjournals.org/content/45/1/8>

Information about reproducing figures, tables, or other portions of this article can be found online at:


<http://jnm.snmjournals.org/site/misc/permission.xhtml>

Information about subscriptions to JNM can be found at:

<http://jnm.snmjournals.org/site/subscriptions/online.xhtml>

The Journal of Nuclear Medicine is published monthly.
SNMMI | Society of Nuclear Medicine and Molecular Imaging
1850 Samuel Morse Drive, Reston, VA 20190.
(Print ISSN: 0161-5505, Online ISSN: 2159-662X)

© Copyright 2004 SNMMI; all rights reserved.

 SOCIETY OF
NUCLEAR MEDICINE
AND MOLECULAR IMAGING